

Properties of plasma fluctuations at the stability threshold: Magnetic well scan in the TJ-II stellarator

A. M. de Aguilera¹, F. Castejón¹, A. López-Fraguas¹, M. A. Pedrosa¹, T. Estrada¹,
M. A. Ochando¹, I. Pastor¹, E. de la Cal¹, C. Hidalgo¹ and the TJ-II Team

¹ Euratom-Ciemat, , Av Complutense 22. 28040 Madrid. Spain

Magnetic well is the main stabilising mechanism in the TJ-II stellarator, since this is an almost shearless device [1]. The magnetic well term must be positive and large enough to compensate the other terms of Mercier criterion [2]:

$$D_M(\rho) = D_W(\rho) + D_S(\rho) + D_I(\rho) + D_K(\rho) \geq 0 \quad (1)$$

The first term in (1) represents the contribution of magnetic well, whose derivative must be positive to be stabilising. TJ-II has the capability to vary its magnetic configuration by changing the currents of its coils, allowing one to change the rotational transform, the plasma volume and shape, almost independently.

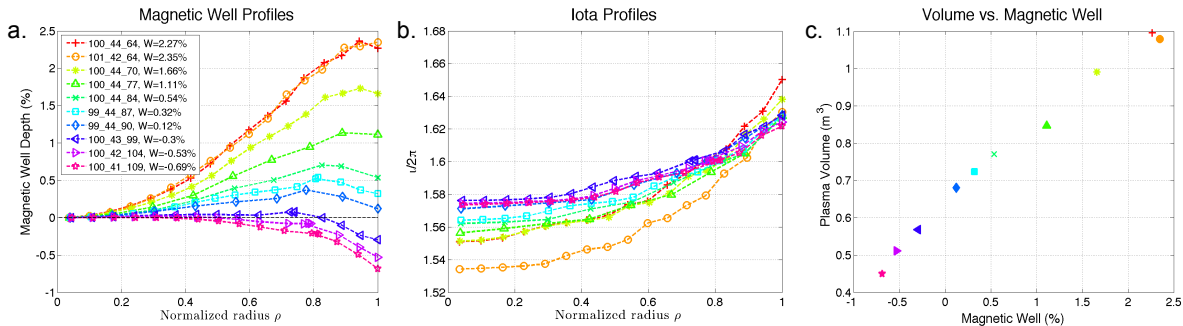


Figure 1: **a.** Magnetic well radial profile. **b.** Rotational transform along normalized radius. The 8/5 rational can be clearly seen around $\rho \approx 0.8$. **c.** Volume for each configuration.

A previous scan [3] between $W = 2.4\%$ and $W = 0.2\%$ performed using ECRH plasmas showed an increase on the turbulent fluxes measured by Langmuir probes. Now the family of ten magnetic configurations shown in Fig 1 has been explored using NBI-plasmas with higher density and lower collisionality. They exhibit, assuming smooth plasma pressure profiles, decreasing magnetic well, from $W = 2.4\%$ to $W = -0.70\%$, at the Last Closed Flux Surface (LCFS) (Fig. 1a.); The rotational transform profile hardly varies around the plasma edge, where the Langmuir probe is going to measure and the 8/5 resonance is located (Fig. 1b.); and a severe decrease in the plasma volume (Fig. 1c.).

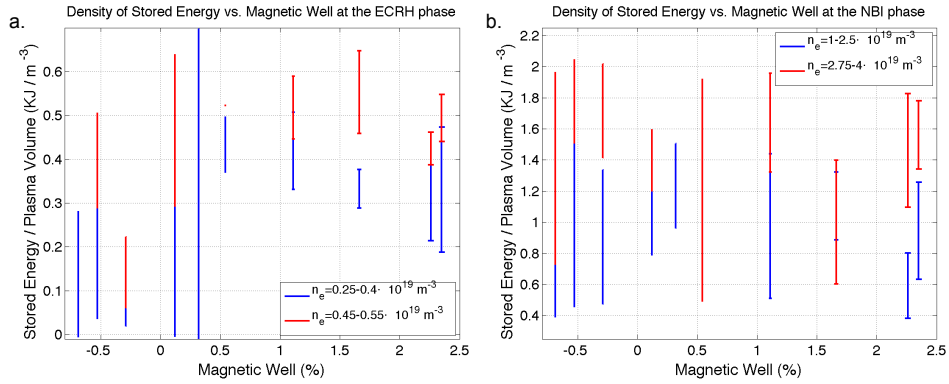


Figure 2: Density of stored diamagnetic energy during **a.** ECRH and **b.** NBI heating.

The reported experiments have succeeded in developing reproducible NBI-heated plasmas for all the configurations; even in the last Mercier-unstable cases. Recall that Mercier criterion is estimated for soft plasma profiles, which could not be the case in real plasmas. Stored diamagnetic energy for certain density values, when divided by each configuration's volume, exhibit little dependency on the magnetic well (Fig. 2): only a clear decrease in density of stored energy is appreciated during the ECRH heating phase, but no trace of it can be found in the NBI cases.

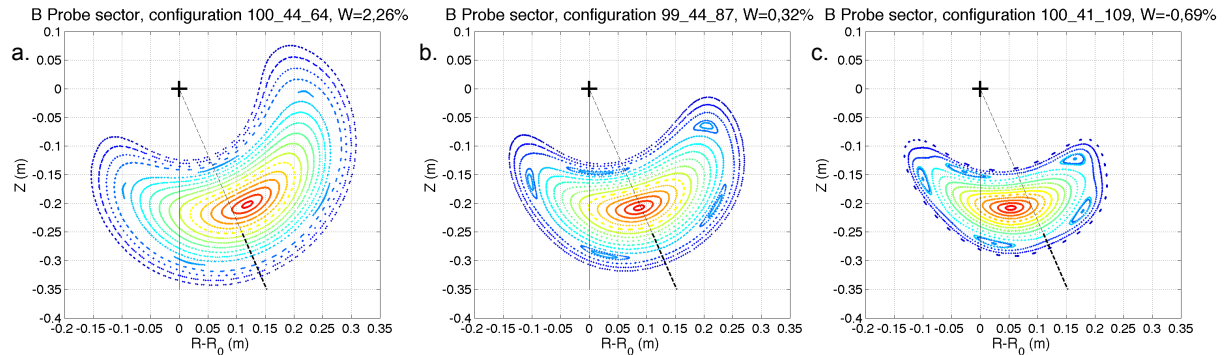


Figure 3: Closed magnetic field lines for three of the explored configurations.

Changes in magnetic topology deform plasma shape during the scan (Fig. 3). In order to compute the energy confinement time for each magnetic configuration, a series of Fafner simulations (Fig. 4a.) were performed to estimate the NBI absorbed power for some of these smaller configurations. Fig. 4b. uses this data to extract the energy confinement time for each case: only in the last three magnetic configurations ($W < 0$ for $\rho > 0.8$) a clear decrease is observed.

The Langmuir probe shown in Fig. 5b. was used in all the experiments. It consists of a rake of eight floating potential pins separated by 1.7mm as shown in Fig. 5a. Plasma access site (Fig. 5c.) allowed to measure at several radial positions for each configuration in order to extract

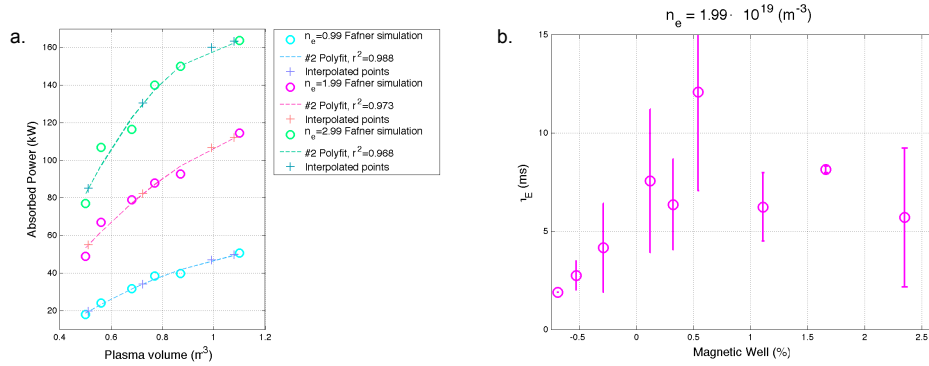


Figure 4: **a.** NBI absorbed power (Fafner simulation) for three possible electron densities, $n_e(0) = 1, 2$ and $3 \cdot 10^{19} m^{-3}$ for different plasma volumes. Non simulated configurations were adjusted by a parabolic fit. **b.** Energy confinement time for $n_e(0) = 2 \cdot 10^{19} m^{-3}$ decreases for the magnetic hill configurations.

detailed floating potential radial profiles.

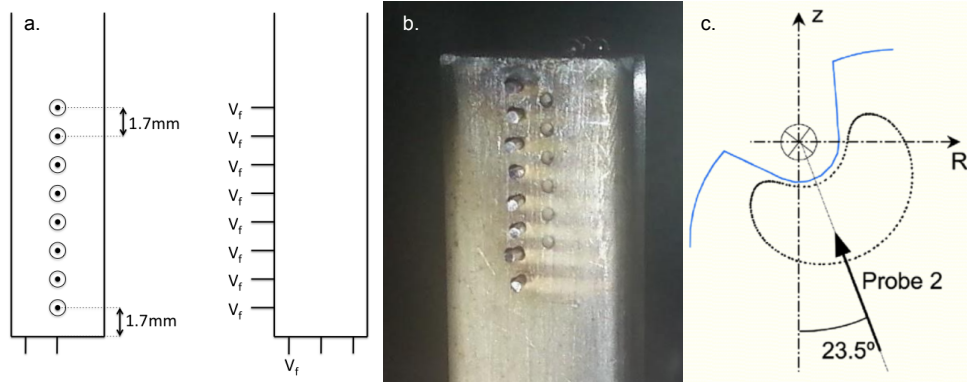


Figure 5: Langmuir probe: **a.** Schematics of the probe system. **b.** Recent photograph of the rake of pins. **c.** Plasma access region.

Such profiles could be extracted for every explored configuration (three of them are shown in Fig. 6a.) so we could compute the shear layer position of each magnetic configuration by searching for the change of curvature of each profile [4]. Fig. 6b. shows that the dependence of this experimental value with the predicted position of the LCFS is approximately linear, showing that this is not affected increase of instabilities.

Once we had confirmed the shear layer location for each configuration, the electrostatic turbulence at that point was studied. First, by analyzing the RMS of the floating potentials at this position (Fig. 7a.); and then running a Fourier Analysis for the signals at the vicinity of this point during NBI (Fig. 7b.) and ECRH (Fig. 7c.) phases. Both procedures suggest that electrostatic turbulence increases significantly in the less stable configurations.

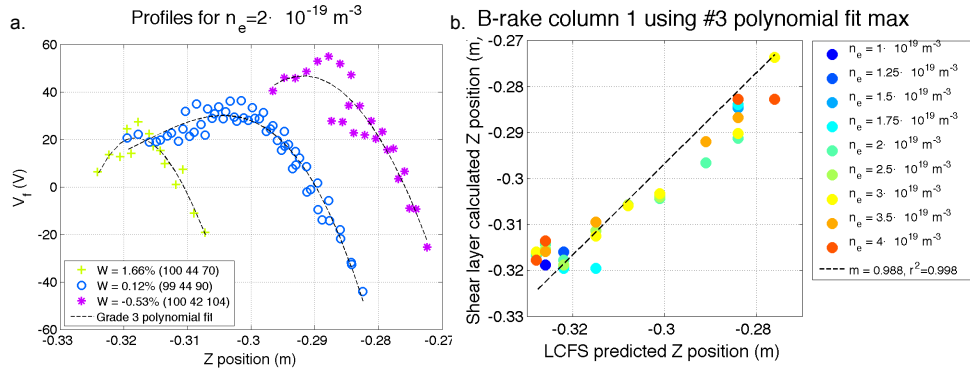


Figure 6: **a.** Selected floating potential profiles for $n_e(0) = 2 \cdot 10^{19} m^{-3}$. Each profile is formed by more than five individual profiles, each of them corresponds to a different Langmuir probe radial position when reproducible plasmas were obtained. **b.** The shear layer position of each configuration lies where the LCFS was predicted by VMEC calculations.

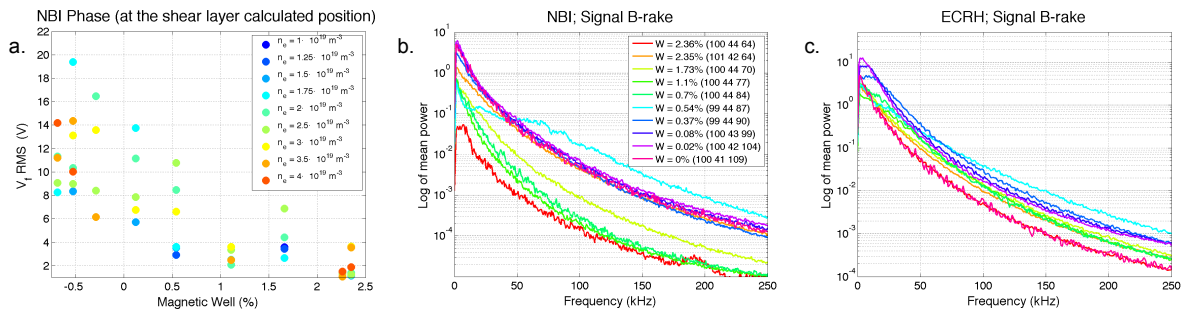


Figure 7: **a.** RMS of the floating potentials at the shear layer increases when we approach the magnetic hill configurations during NBI heating. **b.** Spectrum analysis of the same signals show higher power in the whole frequency range as W decreases. **c.** Same effect during ECRH heating.

This suggest that present stability calculations might miss some stabilization mechanisms like self-organization between transport and gradients [5], which involves a non-linear evolution of the modes [6]. Thus, exploring the impact of relaxing some stability optimization criteria on reactor technology is an important issue for the development of a reactor.

References

- [1] A. Varias, C. Alejaldre et al., Nuclear Fusion **12** 30 (1990)
- [2] V.D. Shafranov. Physics of Fluids **26** 357 (1983)
- [3] J. Castellano, C. Hidalgo et al., Physics of Plasmas **2** 9 (2002)
- [4] C. Hidalgo, J. H. Harris et al., Nuclear Fusion **31** 1471 (1991)
- [5] C. Hidalgo, C. Silva, B. A. Carreras et al., Physical Review Letters **108** 6 (2012)
- [6] K. Ichiguchi and B.A. Carreras. Nuclear Fusion **5** 51 (2011)